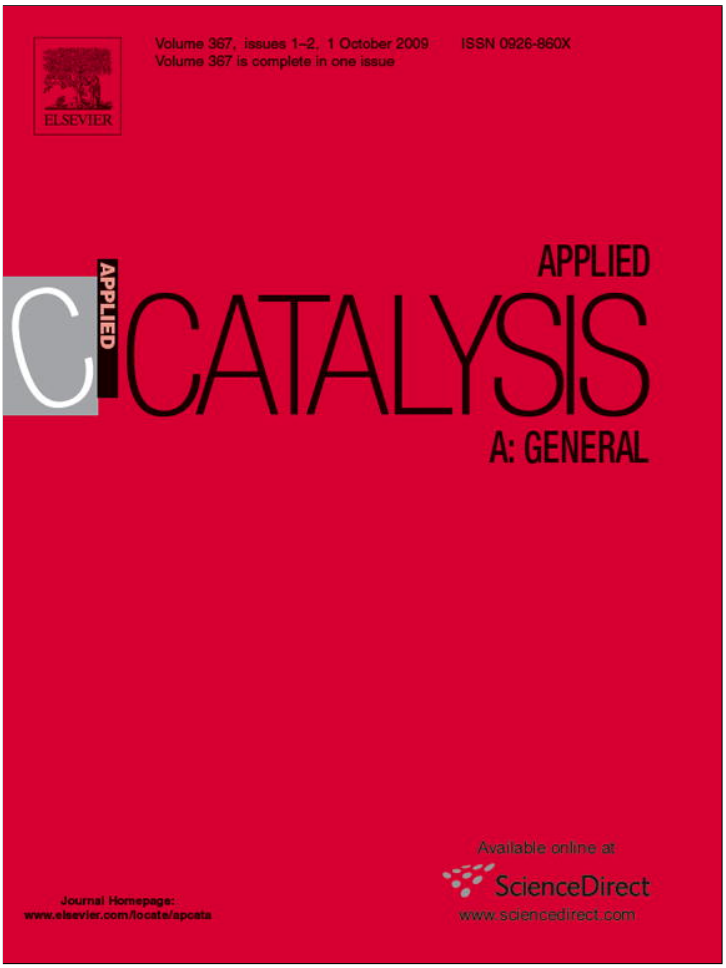

Applied Catalysis A: General 367 (2009) 59–69

Contents lists available at ScienceDirect

Applied Catalysis A: General

journal homepage: www.elsevier.com/locate/apcata

Catalyst formulation to avoid reaction runaway during diesel soot combustion

M.A. Peralta, M.S. Gross, M.A. Ulla, C.A. Querini *

Instituto de Investigaciones en Catálisis y Petroquímica - INCAPE (FIQ, UNL-CONICET) Santiago del Estero 2654, 3000 Santa Fe, Argentina

ARTICLE INFO

Article history:
Received 16 April 2009
Received in revised form 16 July 2009
Accepted 18 July 2009
Available online 25 July 2009

Keywords:
Diesel soot
Reaction runaway
Lanthanum
Cerium
Potassium

ABSTRACT

Soot combustion is a highly exothermic reaction. The aim of this work is to demonstrate that catalyst overheating by reaction runaway can be moderated by the proper selection of a catalyst support, La_2O_3 being a good choice for this purpose. In K/La_2O_3 catalysts, lanthanum compounds decompose in the same temperature range in which soot combustion occurs, thus absorbing part of the heat released in the combustion process and avoiding the reaction runaway. Taking into account this property of catalysts supported on La_2O_3, the catalytic behavior of K/La_2O_3 and K/CeO_2 was compared under reaction conditions in which a reaction runaway could occur. Catalytic activity was followed by temperature-programmed oxidation, and the heats evolved were measured by differential scanning calorimetry. Catalysts were characterized by BET, XRD, DSC and FTIR. Tight and loose contact between catalyst and soot was analyzed, and the effect of NO in the gas phase was studied.

1. Introduction

The use of catalytic filters is one of the alternatives to avoid diesel soot particles and NO_x from being emitted to the atmosphere [1]. The catalyst supported on the filter must be active enough in order to regenerate the filter continuously, thus avoiding an increment in the pressure drop that could lead to engine failure. However, under certain conditions such as when a large amount of soot is accumulated on the catalytic filter, a reaction runaway could occur thus reaching temperatures as high as 1500 °C, which would produce the failure of the catalyst-filter system. In this work, it is shown that the properties found on lanthanum supported catalysts can be useful to lessen the reaction runaway problem. The K/La_2O_3 catalyst has been studied in our group. Several catalytic formulations used for soot oxidation show the beneficial effect of alkaline metals on catalyst activity [2–4]. It has been suggested that these compounds increase the catalyst/soot contact by increasing surface mobility [5,6] and that they favor the oxidation of soot by consuming the carbon to form carbonate species during soot combustion [7]. Many patents reported the use of K in catalysts for soot oxidation [8,9] or catalysts for simultaneous abatement of soot and NO_x [10,11].

We have previously found that lanthanum compounds that are formed in K/La_2O_3 catalysts decompose in the temperature range in which soot combustion occurs [12]. These decomposition processes are endothermic and, therefore, absorbs part of the heat released during the combustion. This leads to a lower total heat release in the soot-catalyst-filter system.

Taking into account this property of La_2O_3 supported catalysts (exothermic and endothermic processes acting simultaneously), the soot combustion reaction was studied under runaway conditions, using the K/La_2O_3 catalyst. The objective is to determine if this catalytic formulation can avoid the great temperature increase that could occur in case of a reaction runaway. Results are compared with those obtained with K/CeO_2 catalysts, which do not exhibit this behavior. Different potassium precursors (nitrate and hydroxide) are study, to analyze the effect of this variable on the phenomena under study. Both, loose and tight contact modes are analyzed, and the effect of NO in the gas phase is also taken into account.

Catalyst stability is beyond the scope of this work. In the case of the catalyst supported on CeO_2 we recently published a detailed study regarding stability at high temperatures, presence of water, SO_2, and CO_2 [2]. Regarding K/La_2O_3 catalyst stability, results concerning thermal stability which are relevant to this study are included.

2. Experimental

2.1. Catalyst preparation

The catalysts were prepared by wet impregnation of KOH or KNO_3 0.1 M solutions on the CeO_2 (Sigma) or La_2O_3 (Alpha) supports. The potassium contents used in this study were 4.5 wt% for the catalysts prepared from KOH and 7 wt% for the catalysts prepared from KNO_3. Each mixture was evaporated while stirring

* Corresponding author. Tel.: +54 342 4533858; fax: +54 342 4531068.
E-mail address: querini@fiq.unl.edu.ar (C.A. Querini).

0926-860X/$ – see front matter © 2009 Elsevier B.V. All rights reserved.
doi:10.1016/j.apcata.2009.07.027

until a paste was obtained. The paste was dried in a stove at 120 °C overnight. The catalysts were calcined at 400 °C during 2 h. The K/La_2O_3 was also calcined at 800 °C, with the purpose of verifying the thermal stability of these catalysts. La_2O_3 may have very different compositions depending upon the pretreatment and precursors used in the preparation. Nevertheless, to simplify the nomenclature, throughout this work catalysts supported on La_2O_3 are designated as KNO_3/La_2O_3 or KOH/La_2O_3, regardless the exact support composition.

2.2. Soot preparation

The soot used in this work was prepared by burning commercial diesel fuel (Repsol-YPF, Argentina) in a glass vessel. After being collected from the vessel walls, it was dried in a stove for 24 h at 120 °C. Its specific surface area was 55 m^2/g. Temperature-programmed experiments performed using helium as carrier gas provided information regarding the amount of partially oxidized groups of the soot surface that decomposes at high temperatures and the amount of hydrocarbons that could remain adsorbed after the diesel combustion. In this way, by heating in an inert gas it was determined that the amount of carbon released as CO, CO_2 and hydrocarbons was 9.3% of the soot [13].

2.3. Activity measurement: temperature-programmed oxidation (TPO)

The catalytic activity was measured by TPO of catalyst–soot mixtures using 20:1, 10:1 and 5:1 mass ratios (the first number represents the catalyst mass and the second number, the soot mass). The soot and the different catalysts were mechanically mixed in an agate mortar for 6 min so as to obtain an intimate contact between them (*tight contact*) [14,15]. In the TPO analysis the following conditions were used: a gaseous mixture of 6% O_2 in N_2 as a carrier gas, with a flow rate of 40 ml/min and a heating rate of 12 °C/min. In this work, a modified TPO technique was used [16] which consists in circulating the gases from the reactor outlet to a methanation reactor, where CO, CO_2 and hydrocarbons are converted into CH_4. Then, CH_4 is continuously measured by an FID detector. The methanation reactor contains a Ni catalyst and operates at 400 °C. Under these conditions (400 °C, 6% O_2, 40 ml/min) a 100% of conversion of CO_x to CH_4 was measured. In order to determine catalyst selectivity, the CO_x production was followed by GC analysis, combining a chromatographic column to separate CO from CO_2, and the methanation reactor. In this way, both components are individually detected by FID with higher sensitivity. The selectivity of the soot combustion reaction to CO_2 was approximately 99 and 97% for the K/CeO_2 and the K/La_2O_3 catalysts, respectively. Due to this very high selectivity to CO_2, all the experiments have been carried out using the methanation technique, since it has higher resolution and sensitivity, and on the other hand, the small amount of CO that could be produced is not relevant to this study. If hydrocarbons desorb at low temperature, they contribute to the FID signal. At higher temperatures, e.g. above 300 °C, the hydrocarbons are burnt on the catalyst and released as CO_2.

It has to be taken into account, that when the reaction runaway occurs, a very fast signal change takes place, and the methanation technique is particularly useful under these conditions, since it provides a continuous monitoring of the (CO + CO_2) being produced.

Activity experiments were carried out using two different reactor configurations. In one of them three thermocouples were used. The reactor used in this case was a straight tubular reactor. The first thermocouple was located between the reactor wall and the oven wall, and was used as the control thermocouple. A second thermocouple was located directly in the bed, well at its middle position. This thermocouple was positioned in the bed without using a glass well, in order to avoid an excessive mass (glass and thermocouple) that could interfere with the temperature being measured. The third thermocouple was located directly underneath the bed, to monitor the temperature of the gases coming out of the catalytic bed.

In the other configuration, the reactor used for the TPO analysis was a U-type reactor. In one of its branches, the catalytic bed was placed. The other arm contained the thermocouple, which was placed at the same height as the catalytic bed. This thermocouple therefore indicates the temperature that the catalyst bed should have if there were no energy transfer limitations, such as a local heating of the bed due to the exothermic effect caused by the reaction. Under this configuration, no perturbation of the catalytic bed takes place due to the sensor element, which for a laboratory scale will have a dampening effect on the temperature increase when observing a runaway phenomenon. It has been determined by simulation calculations, that for typical activation energies found for the soot oxidation reaction, the reaction rate should not change faster than 0.2 mol s^{-1} K^{-1} [28] if the system is working in a kinetic controlled regime, and no energy transfer limitations occurs. Therefore, the data obtained during a TPO can be used to quantitatively asses if the system if having a reaction runaway, without measuring the bed temperature.

The sample mass loaded into the cell was always 10 mg, and therefore the amount of soot loaded in each experiment was 0.47, 0.91 and 1.67 mg for catalyst:soot mass ratio of 20:1, 10:1 and 5:1, respectively.

The combination of these two different experimental set-ups makes it possible to obtain enough data to understand the phenomena, and also to verify the validity of simplified models in order to reproduce the experimentally observed TPO profiles. Results are presented in order to demonstrate that both configurations are providing reliable and equivalent information regarding the phenomena under study.

2.4. Differential scanning calorimetry (DSC)

The endothermic evolutions (in this case, phase decompositions) and exothermic evolutions (soot combustion) that take place as a temperature ramp was applied, were measured by DSC using synthetic air as a carrier gas, with a flow rate of 90 ml/min and a heating rate of 10 °C/min. For the DSC analysis, 10 mg of catalyst or 10 mg of catalyst–soot mixture (same as in the TPO experiments) were placed in an aluminum crucible. The catalyst–soot mixtures were the same as those used in the TPO analysis. The DSC analyses were carried out in a DSC821e Metler Toledo equipment. Experiments were also carried out using 10%CO_2/5%O_2/balance N_2.

2.5. Catalyst characterization

The catalysts used in this work were characterized by FTIR, XRD and DSC. Infrared spectra were obtained at room conditions using a Shimadzu 8101M spectrometer. Samples were prepared in the form of pressed wafers (ca. 1% sample in KBr). All spectra involved the accumulation of 80 scans at 4 cm^{-1} resolution. The X-ray diffractograms were obtained with a Shimadzu XD-D1 instrument with monochromator using Cu Kα radiation at a scan rate of 1°/min, from $2\theta = 20°$ to 100°. DSC analyses of pure catalysts were carried out as above described.

The BET surface area was determined using a Quantachrome Nova 1000 sorptometer.

2.6. TPO simulation

In order to obtain additional information regarding the phenomena under analysis, and to determine reaction rate changes

and oxygen consumption during reaction, a simplified model has been used, as described in [17], using a model with a power law kinetic, considering that:

- The soot reaction order is, as an average, one or less than one.
- The oxygen reaction order is one.
- There are different contributions to the overall CO_2 generation, due to reaction of soot with different catalytic sites and/or to catalyzed and non-catalyzed reactions. Each of these contributions has different activation energies and pre-exponential factors. The parameters for this model are estimated by regression of the experimental data.

The objective of using this very simple model, which has been applied for this reaction system in many studies [18–27], is only to verify if the observed temperature increment is consistent with normal global activation energies as used in this model, and also to calculate the oxygen consumption to determine whether this can affect the TPO profile. Since the O_2 consumption is only due to the CO_2 formation (and a very small amount of CO) by soot burning, the model can predict O_2 concentration along the catalyst bed with very little uncertainty, enough to determine if the concentration is depleted to levels in which it may control the oxidation kinetics.

2.7. TPO experiments in the presence of NO and loose contact

TPO experiments were carried out as above described, but using 1000 ppm of NO in air. Since NO is transformed either to N_2 or to NH_3 in the methanation reactor, and any of these are not detected by the FID, it is possible to follow the activity continuously with the same configuration, thus improving the detection resolution and sensitivity.

Different types of contacts between the catalyst and the soot were used to perform these experiments. Mixtures with loose contact were prepared just shaking the catalyst and the soot in a vial, which is the method typically used in laboratory studies. This loose type of contact is not completely realistic either, since in a real application the level of contact between the soot and the supported catalyst will be in between the *loose* and the *tight* contact as used in this work. Therefore other mixtures were prepared. In these cases, the catalyst and the soot were mixed in a mortar for few seconds, using different mixing times.

3. Results

The conditions under which a runaway was possible during soot combustion in laboratory experiments were previously found [28]. In brief, using a mixture of 5 weight parts of catalyst and 1 part of soot (5:1 ratio), the runaway could take place depending on the catalyst activity. Instead, using a mixture of 20 parts of catalyst and 1 part of soot (20:1 ratio) the runaway was not observed with any of the catalysts studied.

3.1. BET Surface area

The CeO_2 support has a low surface area of 7.6 m^2/g. This value decreased to 3.3 and 2.3 m^2/g after preparation of KOH/CeO_2 and KNO_3/CeO_2, respectively. Similar behavior was found with La_2O_3 as support, being 9.2 m^2/g its initial BET area, and decreased to 4 and 3.8 m^2/g after preparation of KOH/La_2O_3 and KNO_3/La_2O_3, respectively.

In this system, only the external surface is used since the soot particles are bigger than the pore size. Both solid have very similar values of BET area, and therefore it can be expected that this property will not introduce different behaviors between these catalysts, regarding a possible runaway during soot combustion.

3.2. DSC measurements

In Fig. 1A and B DSC results are shown for the $KOH(4.5)/CeO_2$ and $KOH(4.5)/La_2O_3$ catalysts, respectively. Both figures show the heats evolved during the combustion of catalyst:soot mixtures with 20:1, 10:1 and 5:1 mass ratios. Comparing the profiles for the 20:1 mixtures, it can be observed that the DSC profile for the $KOH(4.5)/CeO_2$ catalyst (Fig. 1A) is thinner and higher than the $KOH(4.5)/La_2O_3$ profile (Fig. 1B). Observe that the maximum heat power, is ca. 17 mW for $KOH(4.5)/CeO_2$ and ca. 8 mW for KOH(4.5)/

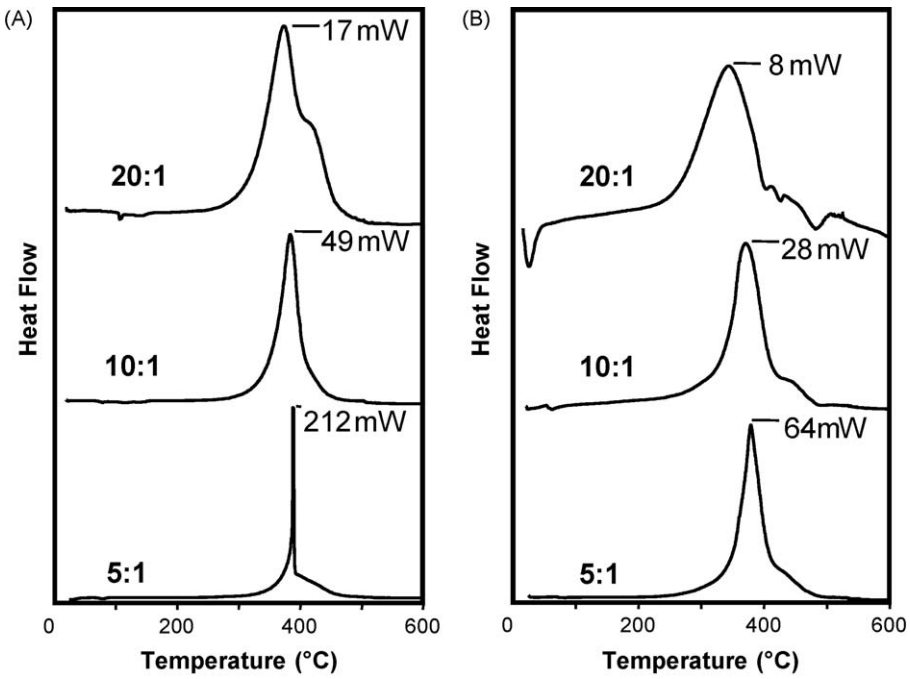

Fig. 1. DSC profiles for catalysts:soot mixtures with mass ratios of 20:1, 10:1 and 5:1. (A) $KOH(4.5)/CeO_2$ calc. 400 °C and (B) $KOH(4.5)/La_2O_3$. Catalysts calcined at 400 °C.

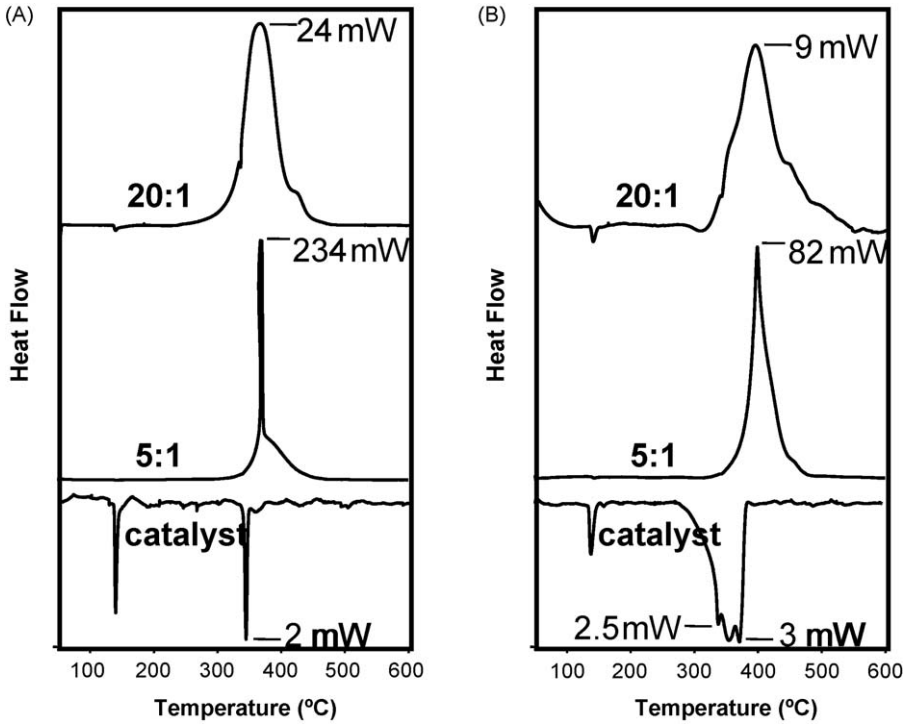

Fig. 2. DSC profiles for the catalyst and catalyst:soot with mass ratios of 20:1 and 5:1: (A) $KNO_3(7)/CeO_2$ and (B) $KNO_3(7)/La_2O_3$.

La_2O_3. The activity is similar in both cases, as indicated by the temperature range in which the soot is burned.

Comparing the DSC profiles for the 5:1 mixtures of both catalysts, it can be observed that a runaway occurs with the $KOH(4.5)/CeO_2$ catalyst (Fig. 1A), and does not occur with the $KOH(4.5)/La_2O_3$ catalyst (Fig. 1B). The runaway is detected by observing the DSC profile shape, and using the value of the slope of the TPO curves, which should not be significantly higher than 0.2 mol s^{-1} K^{-1}, the DSC profile for the 5:1 mixture with the $KOH(4.5)/CeO_2$ catalyst is very thin and high, which is consistent with a fast heat generation during the combustion reaction. Under this condition, the rate of heat generation by the combustion is much higher than the rate of heat dissipation. The DSC profile presents a vertical slope, which would mean that the reaction rate would be increasing at a very high rate at constant temperature, which is unlikely under a kinetic controlled regime. Obviously, what is happening is a local temperature elevation in the mixture, which leads to a reaction acceleration and therefore to a very fast heat release, as indicated by these experiments with the DSC. This clearly indicates that the system is operating in an energy transference controlled regime, with a strong local heating and the consequent increase in the reaction rate. The maximum heights (catalyst:soot mass ratio = 5:1) for the DSC profiles are approximately 212 mW for $KOH(4.5)/CeO_2$ catalyst and 64 mW for $KOH(4.5)/La_2O_3$ catalyst. Note that, besides the height, the profile shape for the 5:1 mixture with $KOH(4.5)/CeO_2$ is characteristic of those cases in which a runaway occurs, and is different from that of the $KOH(4.5)/La_2O_3$ catalyst.

Experiments with K/CeO_2 and K/La_2O_3 catalysts, prepared using KNO_3 as precursor, were also performed. Fig. 2A and B shows the DSC profiles for the mixtures of these catalysts and soot (20:1 and 5:1 catalyst:soot mass ratios). The DSC profile obtained with the catalyst without soot is also included. The profiles are shown in different scales in order to observe them clearly. The maximum power release is indicated for each profile. Again, it can be observed that the reaction runaway occurs in the presence of $KNO_3(7)/CeO_2$ and not in the presence of $KNO_3(7)/La_2O_3$. Comparing these profiles with those obtained with the catalysts prepared from KOH (Fig. 1A and B), it can be observed that the DSC curves are sharper for the catalysts prepared from KNO_3.

Heat values evolved during these experiments are summarized in Table 1. These values were obtained by integration of the DSC profiles shown in Fig. 2. Table 1 includes DSC results obtained with catalyst:soot mixtures with a 5:1 mass ratio using air as carrier gas, as well as a carrier gas containing 10%CO_2 in 5%O_2/N_2. It can be seen that the presence of CO_2 does not affect the amount of heat consumed by the system significantly to decompose the hydroxyl groups. Also, a $KNO_3(7)/La_2O_3$ catalysts was mixed with soot, pretreated in N_2 at 400 °C to dehydroxylate the support, and then the DSC experiment was carried out. It can be seen in Table 1 that the heat evolved agrees very well with that found on $KNO_3(7)/CeO_2$.

3.3. TPO analyses in the U-shape reactor

Fig. 3A and B shows the TPO profiles for the mixtures used in the DSC experiments of Fig. 1A and B, respectively. The TPO profiles for the different mixtures are not in the same scale, in order to be able to observe each of them clearly. In the case of the $KOH(4.5)/La_2O_3$ catalyst, as the catalyst:soot ratio decreases, the TPO profiles shifts

Table 1
Heat evolved during DSC analyses. Negative values refer to exothermic processes.

Catalyst	Catal./ soot ratio	Carrier in DCS	Total Heat (J/g)
$KNO_3(7)/CeO_2$		Air	8
$KNO_3(7)/CeO_2$	20:1	Air	896
$KNO_3(7)/La_2O_3$		Air	145
$KNO_3(7)/La_2O_3$		10%CO_2–5%O_2–N_2	128
$KNO_3(7)/La_2O_3$	20:1	Air	702
$KNO_3(7)/La_2O_3$	20:1	10%CO_2–5%O_2–N_2	714
$KNO_3(7)/La_2O_3$ dehydroxylated	20:1	Air	843

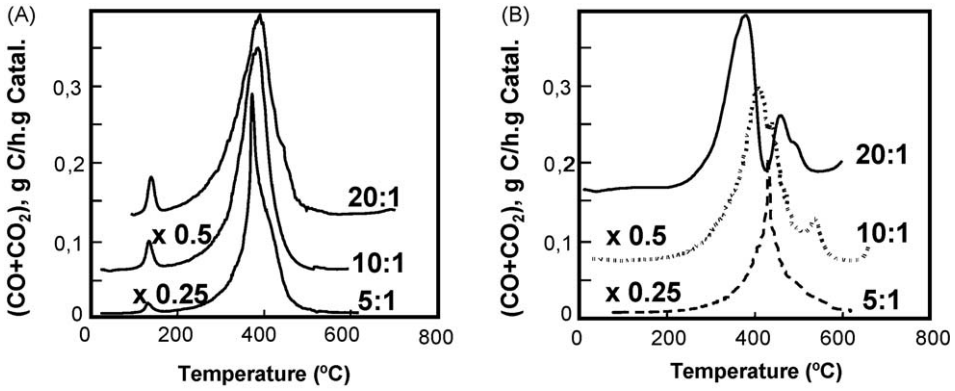

Fig. 3. TPO profiles for mixtures of catalyst:soot with mass ratio of 20:1, 10:1 and 5:1: (A) KOH(4.5)/CeO_2 and (B) KOH(4.5)/La_2O_3.

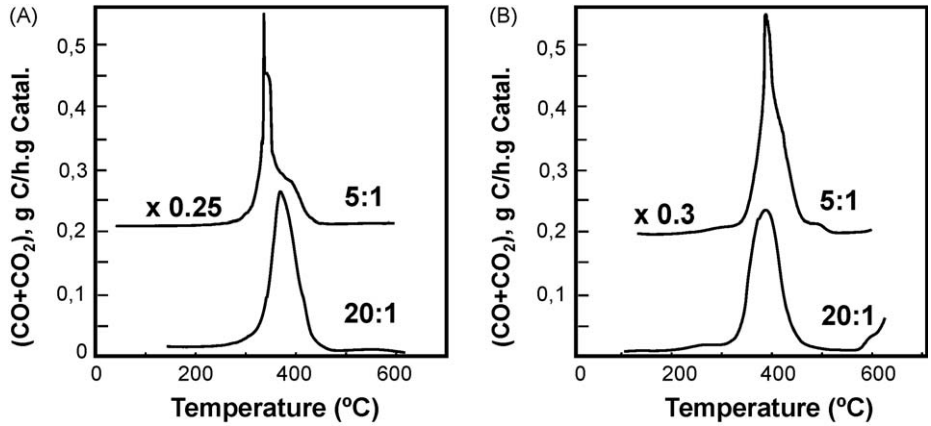

Fig. 4. TPO profiles for 20:1 and 5:1 mixtures; catalyst: (A) KNO_3(7)/CeO_2 and (B) KNO_3(7)/La_2O_3.

to higher temperature. In the case of the KOH(4.5)/CeO_2 catalyst, the opposite behavior was observed.

Fig. 4A and B shows the TPO profiles corresponding to experiments carried out with the same samples used in the DSC analyses shown in Fig. 2A and B, respectively. In the 5:1 TPO profile for the KNO_3(7)/CeO_2 catalyst (Fig. 4A), the typical runaway shape can be observed, which is very similar to that observed in the DSC profile (Fig. 2A). Both techniques, DSC and TPO, make it possible to detect the temperature runaway phenomena. Comparing Figs. 3A and 4A it can also be observed that the TPO profile for the 5:1 mixture with K/CeO_2 prepared with KNO_3 is sharper than the corresponding to the catalyst prepared from KOH. This result suggests that the reaction runaway will be less probable when using catalysts prepared from KOH than when using catalysts prepared from KNO_3. The TPO profile obtained with KNO_3(7)/CeO_2 is sharper than that obtained with KOH(4.5)/CeO_2 mainly because of the precursor, and not because of a higher K loading, as was also previously reported [4].

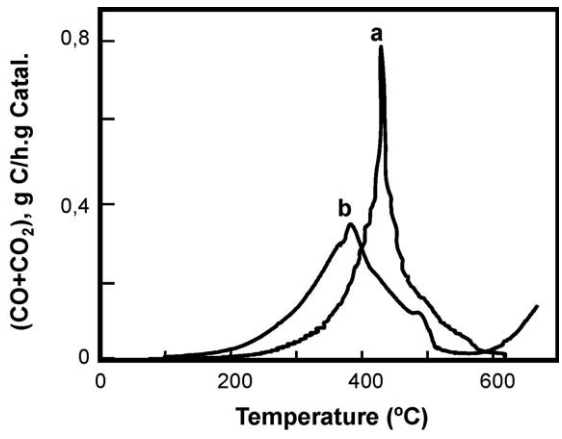

Fig. 5. TPO profiles for the KOH(4.5)/La_2O_3 mixtures with soot (5:1); (a) fresh mixture and (b) aged mixture.

The reason of this is that during impregnation with KNO_3 and calcination, a fraction of the exposed lanthanum hydroxide will be transformed into lanthanum nitrate, which does not decompose in the same temperature range as the hydroxide.

Fig. 5 shows the TPO profiles carried out with a 5:1 mixture with KOH(4.5)/La_2O_3, using two catalyst samples that were stored during different times. One of them is a freshly prepared and calcined catalyst, and the other one was aged by storage during 33 months. The aged catalyst presents a higher proportion of $La(OH)_3$ if compared with the fresh catalyst, as observed by FTIR (see below).

The experiments shown in Fig. 6 provide further evidence about the influence of $La(OH)_3$ in the runaway dampening effect. Fig. 6 shows the TPO profiles for 5:1 mixtures using the KNO_3(7)/La_2O_3 catalyst. The catalyst–soot mixture was the same in all cases but the TPO experiments were carried out in the following manner: (i) 15 days after the catalyst preparation with a dry carrier (curve a), (ii) 15 days after the catalyst preparation with a wet carrier saturated with water at room temperature (curve b), and (iii) 3 months after the catalyst preparation with a dry carrier. It can be observed that only when the catalyst has recently been calcined the runaway could occur, although with a moderate intensity. These results are relevant from an applied point of view, since the engine exhaust gases contain water and this could have an effect in the rate and/or temperature of dehydroxylation. According to

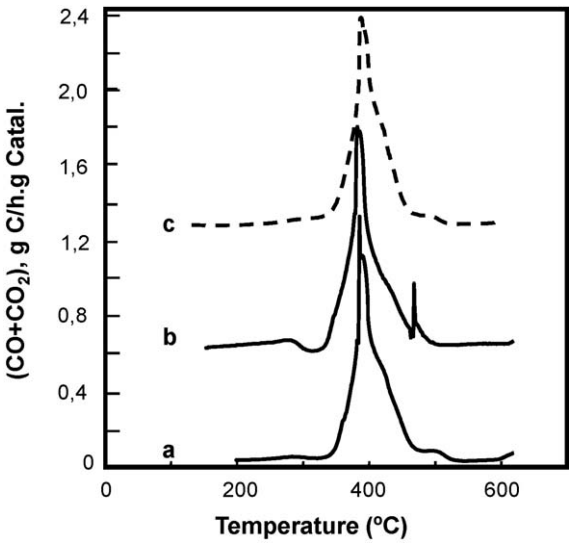

Fig. 6. TPO profiles for 5:1 mixtures with $KNO_3(7)/La_2O_3$ catalyst: (a) fresh catalyst, dry carrier, (b) fresh catalyst, wet carrier and (c) aged catalyst.

these results, the presence of water in the gas phase does not inhibit the decomposition of $La(OH)_3$.

3.4. TPO analyses with bed and gas phase temperature measurement

All the experiments carried out with catalyst:soot ratios of 20:1 or 10:1 yielded the same results regarding the difference among the three measured temperatures: oven wall, catalyst bed, and gas phase downstream the bed. Typically, the difference between the oven wall and the bed temperature was less than 5 °C, while the difference between the bed temperature and the gas phase right below the catalytic bed increased as a function of the temperature. Initially, e.g. below 50 °C there is no difference; when the bed temperature is at 100 °C, the gas temperature is 3 °C lower, and this difference gradually increases being approximately 15 °C when the bed temperature is 400 °C, and between 16 and 18 °C at 600 °C. This is because at higher temperatures, the pre-heater zone is not enough to increase the gas from room temperature up to the bed temperature, and therefore the gas is a little cooler than the bed.

Fig. 7 A shows the TPO profile for a KNO_3/CeO_2 catalyst, mixed with soot in a 5:1 mass ratio. Fig. 7B shows a detail of the bed temperature at the moment in which the runaway phenomena occurred. It can be seen that the sudden increase in temperature for this small catalytic bed of 10 mg, is more that 30 °C, in spite of the thermocouple that dampened the effect of the exothermicity of the reaction. All the experiments shown in Figs. 3 and 4 were repeated with this configuration. Since the results are exactly the same as those shown in Figs. 3 and 4, only one example is presented (Fig. 7).

Table 2
XRD and IR analyses. Phases found in the catalysts used in TPO and DSC experiments.

Catalyst	DRX	IR
La_2O_3, just bought	La_2O_3, $La(OH)_3$, $La_2O_2CO_3$	$La(OH)_3$, $La_2O_2CO_3$
La_2O_3, aged	$La(OH)_3$, $La_2O_2CO_3$ (traces)	$La(OH)_3$, $La_2O_2CO_3$ (traces)
KOH/La_2O_3	$La(OH)_3$, $La_2O_2CO_3$	$La(OH)_3$, $La_2O_2CO_3$
KNO_3/La_2O_3	$La(OH)_3$, $La_2O_2CO_3$, KNO_3 traces	$La(OH)_3$, $La_2O_2CO_3$, KNO_3
KOH/CeO_2	CeO_2	
KNO_3/CeO_2	CeO_2, KNO_3 (traces)	KNO_3
KNO_3/CeO_2 aged	CeO_2, KNO_3 (traces)	KNO_3

It has to be emphasized that the difference in the temperature between the oven and the catalytic bed was only observed when loading a 5:1 catalyst to soot mass ratio with CeO_2 supported catalysts. In all the other experiments, the oven and the bed temperature were practically the same and the gas phase temperature downstream the bed was a few °C lower.

3.5. Catalyst characterization

Table 2 summarizes catalysts characterization results, regarding phases as detected by XRD, and species as detected by FTIR.

Fig. 8 shows XRD patterns for fresh and aged La_2O_3, and for aged La_2O_3 right after calcination. Ageing occurred just by storing the sample in normal conditions after opening the original container. It can be clearly seen that there is a very strong signal due to the $La(OH)_3$ phases after exposing the sample to ambient air. After calcination, these phases partially disappear. Fig. 9 shows the FTIR spectra of the same samples, fresh and aged at ambient conditions. These results agree with those found by XRD, i.e., a large increase in the amount of $La(OH)_3$ is observed upon contacting the material with the ambient and therefore humid air. The same XRD and FTIR phases were found when adding KOH to the catalyst.

In the case of the CeO_2 supported catalysts, no significant differences where observed by XRD and FTIR upon catalyst ageing (spectra not shown).Fig. 2 A and B shows the DSC results for the pure catalysts (without soot). In both of them (K/CeO_2 and K/La_2O_3) endothermic processes take place while heating in a dry gas (O_2/N_2). The first peak (approximately at 130 °C) is assigned to water desorption. The KNO_3 melting point is 344 °C; thus the peak at 340 °C is assigned to nitrate melting. This peak was not observed when using KOH as the potassium precursor, which also supports this assignment. We have reported [12] that the DSC profile corresponding to KOH/La_2O_3 presents an endothermic peak at 380 °C assigned to the $La(OH)_3$ decomposition, also based on the DSC analysis of pure $La(OH)_3$ is previously reported [29]. In the case of the lanthanum supported catalyst, the broad signal that comes out between 300 and 400 °C, partially overlaps that of nitrate melting.

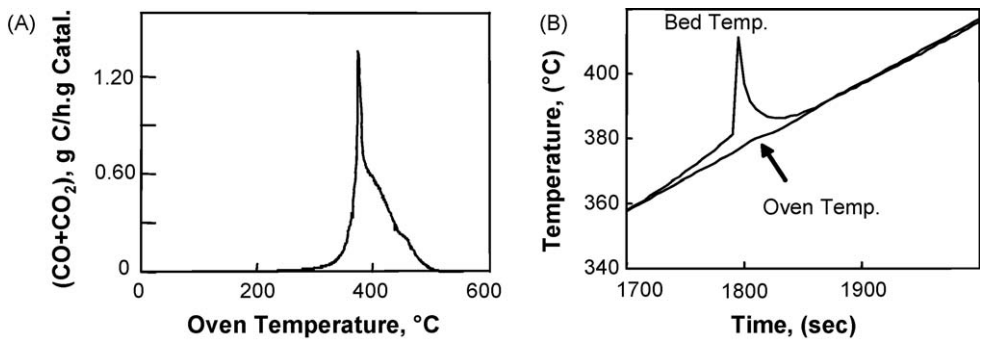

Fig. 7. (A) TPO profile for $KNO_3(7)/CeO_2$ mixed with soot (5:1). (B) Detail of temperature evolution in the catalytic bed during the reaction runaway.

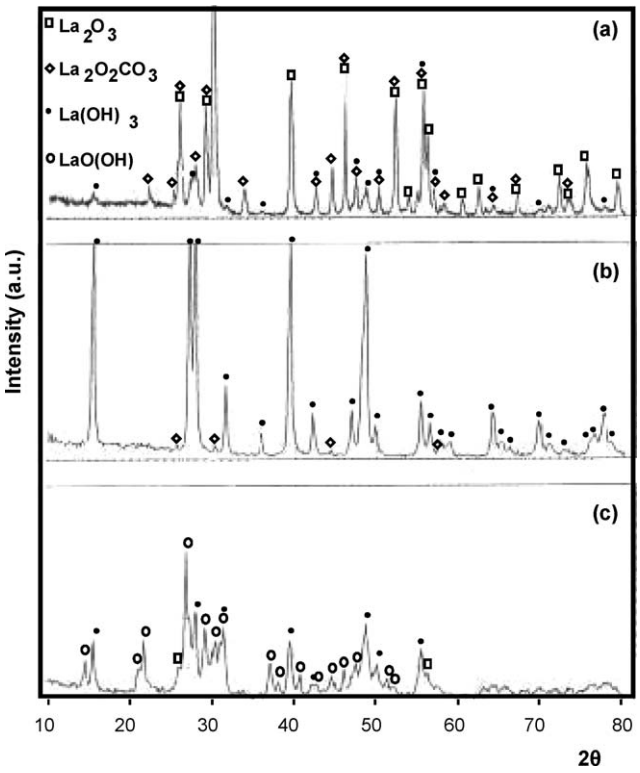

Fig. 8. XRD patterns for La_2O_3 solids: (a) just bought; (b) aged; (c) aged and calcined at 400 °C.

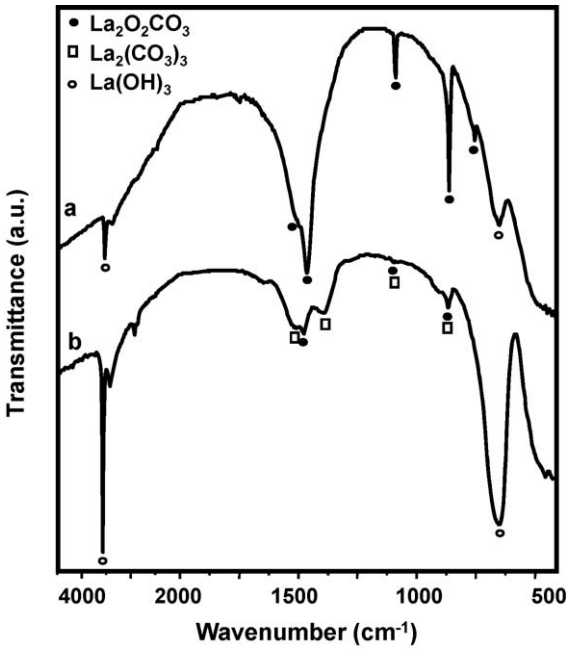

Fig. 9. FTIR spectra for (a) just bought La_2O_3 and (b) aged La_2O_3.

3.6. TPO simulation

Fig. 10 shows an example of the TPO profile obtained with the above simplified model described in Section 2.6, in order to determine whether the observed total rate of combustion is consistent with the temperature increase detected in the catalyst bed. The simulation was carried out using the experimental bed temperature, shown in Fig. 7. Fig. 10A shows the simulated TPO profile, using the experimental temperature data, and using 3 peaks to deconvolute the overall signal, with activation energies of 39, 41 and 43 kcal/mol K. Fig. 10B shows the oxygen composition as a function of time, in different positions along the bed. It can be clearly seen how the reaction depletes the oxygen along the bed at this high soot content (catalyst:soot = 5).

3.7. Catalysts stability

It has been shown that Ba, K/CeO_2 catalysts displays very good thermal stability [2]. The activity for soot burning is the same for calcination temperatures between 400 and 830 °C, with the same TPO profile. This shows that the catalyst can tolerate high temperature excursions without loosing activity and, therefore, its behavior regarding the possibility of having a reaction runaway will not be affected by short treatments at high temperature.

The K/La_2O_3 catalyst calcined at 800 °C during 2 h, mixed with soot in a ratio 20:1 displays a TPO profile (not shown) similar to that of the catalyst calcined at 400 °C, shown in Fig. 3B. The temperature at which the maximum occurs is 380 °C, while with the catalyst calcined at 400 °C the maximum is at 365 °C. It means that there is a small activity loss upon treatment at high temperatures.

4. Discussion

4.1. Phases transitions

La_2O_3 displays a complex and interesting behavior regarding the surface and bulk composition. For $La(OH)_3$ as starting solid, Taylor and Schrader [31] found the following phases: $La(OH)_3$ and $[CO_3^{2-}]$ after heating at 200 °C; LaO(OH), $[La_2O_2CO_3]$ and $[La_2O_3]$ after heating at 400 °C; La_2O_3 and $[La_2O_2CO_3]$ after heating at 600 °C. Minor phases are indicated between brackets. In the case of $La_2O_2CO_3$, no phase transformation occurred until 700 °C. Milt et al [12] found that the changes on surface composition on K/La_2O_3

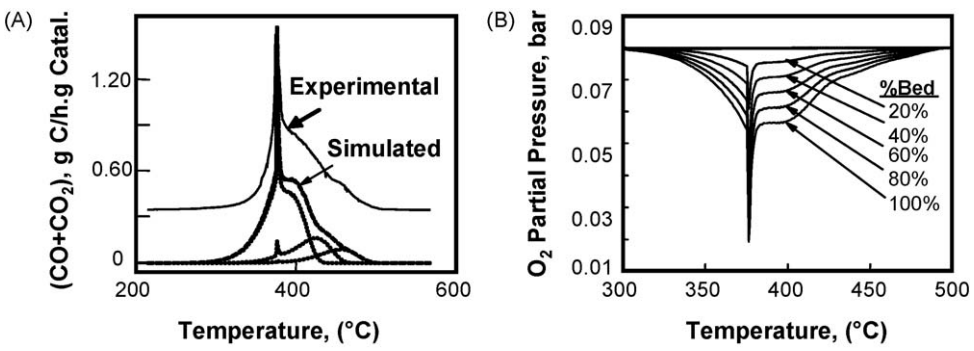

Fig. 10. (A) Simulated TPO profile using the temperature data from Fig. 7 and (B) oxygen concentration profiles during the TPO analyses, calculated with the simulation model.

upon treatment in dry air are as follows: $La(OH)_3 \rightarrow LaO(OH)$ between 300 and 400 °C; $LaO(OH) \rightarrow La_2O_3$ between 400 and 550 °C; $La_2O_2CO_3 \rightarrow La_2O_3$ and $2KNO_3 \rightarrow K_2O + 2NO_2$ between 550 and 800 °C. The decomposition of lanthanum carbonates starts approximately at 460 °C [32] as follows: $La_2(CO_3)_3 \rightarrow La_2O_2CO_3 + 2CO_2$.

As indicated in Table 2, and Figs. 8 and 9, the catalysts supported on La_2O_3 easily form $La(OH)_3$, which also decomposes upon calcination at 400 °C. This was clearly indicated by the XRD spectra of the aged catalyst, before and after treatment at 400 °C. Fig. 2A and B shows the DSC of the pure catalysts (without soot). It can be observed that the DSC profile obtained with $KNO_3(7)/La_2O_3$ without soot presents an endothermic peak with a maximum heat absorption at 380 °C, corresponding to $La(OH)_3$ decomposition, as mentioned above. In the $KNO_3(7)/CeO_2$ profile (Fig. 2A) the endothermic peak at about 340 °C was assigned to the KNO_3 melting. It has to be emphasized that KNO_3 is present on these catalysts after calcination, as it was detected by XRD and FTIR (see Table 2).

Note that above 400 °C and up to 600 °C, no signals are displayed on the DSC profiles even though the calcination temperature was 400 °C. Therefore, there is no phase transition in this temperature range and no interference with the soot combustion signal might be expected. TPO carried out to pure catalysts recently calcined (not shown), also did not show signals that might overlap the profile corresponding to coke burning.

4.2. Phase transitions and soot combustion

The endothermic evolution due to lanthanum dehydroxylation takes place in the same temperature range as the exothermic soot combustion, particularly close to the maximum burning rate. Consequently, the net heat released during soot combustion will be lower in the case of KOH/La_2O_3 compared with the KOH/CeO_2 catalyst, since the latter does not experiment any endothermic process in this temperature range, as observed in a KOH/CeO_2 DSC profile up to 600 °C (not shown). The runaway takes place when the heat generation rate is above a given threshold for a given system. Therefore, the temperature range in which the exothermic and the endothermic processes take place will determine if the system could have the temperature runaway. If both processes take place simultaneously, the runaway might not take place if the endothermic process consumes enough amounts of heat. This would be the ideal situation in order to design a catalytic system with self-regulated reaction temperature. The nitrate decomposition observed in the case of $KNO_3(7)/CeO_2$ is only 8 J/g, while the dehydroxylation of $KNO_3(7)/La_2O_3$ corresponds to a heat consumption of about 145 J/g (see Table 1). The latter is strongly affected by the degree of hydroxylation of the catalyst, and therefore could be even higher than this value. It was shown [30] that the degree of hydroxylation of the $KNO_3(7)/La_2O_3$ catalyst aged 3 years is considerably higher than the one corresponding to the catalyst aged 8 months, simply due to the exposure to the environment. The endothermic evolution corresponding to the KNO_3 melting process occurs at a temperature lower than the temperature range where a high rate of heat release occurs during soot combustion and, therefore, it has no dampening effect. Also, the total heat absorption by the nitrate melting is a low fraction of the total heat evolved in the combustion. Therefore, although KNO_3/CeO_2 catalysts with a load of 4.5% of K were not evaluated, the KNO_3 melting process will not damp the reaction runaway at this low potassium content, since at a higher loading level (7 wt%) the heat consumed by the melting process is not enough to mitigate the runaway.

The data shown in Table 1, clearly indicate the relevance of the heat consumed by the dehydroxylation, as compared to the total heat release due to soot combustion. Note that in the case of the KNO_3/CeO_2 the total heat release is 896 J/g, and the endothermic processes detected on this catalyst (see Fig. 2A) involved only heat absorption of 8 J/g. On the other hand, with the KNO_3/La_2O_3 catalyst, the endothermic process due to dehydroxylation involves 145 J/g, which is a significant fraction of the total heat release due to soot combustion. Note that in this case, the total heat release (702 J/g) which is the result of the exothermic combustion plus the endothermic decomposition is correspondingly lower than that observed with ceria as support (896 J/g). The DSC experiment carried out after pretreating the mixture (soot + $KNO_3(7)/La_2O_3$) in N_2, perfectly agrees with above discussion. In this case the total heat evolved was 843 J/g, while the non-pretreated catalyst liberated a total of 702 J/g, being the heat consumed by dehydroxylation 145 J/g. If these two values are added, a combustion heat of 847 J/g are obtained, in complete agreement with the 843 J/g measured for the dehydroxylated catalyst.

It is an important observation that the soot burning process takes place in the same temperature range for both catalysts, and in spite of this, the runaway is observed in one catalytic system, and not in the other.

4.3. Kinetics effects

Fig. 3B shows that there is a shift towards higher temperatures as the catalyst:soot ratio decreases. Since the same (catalyst + soot) mixture mass was loaded in all the experiments, the soot mass charged was the highest when the catalyst/soot ratio was the lowest. In these cases, there is a higher oxygen uptake decreasing the oxygen partial pressure, which reduces the reaction rate shifting the TPO profile to higher temperatures [17]. Fig. 10B shows the oxygen concentration along the bed, in the case of a catalyst:soot ratio of 5:1, where a runaway took place. These values were obtained by calculation, using the simulation model and the experimental temperature evolution shown in Fig. 7B. There is a significant decrease in the oxygen concentration along the bed and, therefore, a decrease in the reaction rate can be expected when higher oxygen consumptions take place. This is the reason why the TPO profile shifts to higher temperatures, as the catalyst:soot ratio decreases, as long as no runaway takes place. This agrees with experimental results previously reported [28]. In this latter study, the effect of the carrier gas flow rate was analyzed. It was found that increasing the flow rate and consequently the oxygen supply, the TPO profile shifts to lower temperatures. Other results that support this conclusion, was obtained by loading mixtures with different contents of carbon, but in order to have exactly the same amount of carbon loaded into the cell. Under this condition, no shift in the TPO profile was observed [17]. Simulations results previously reported also support these comments [17,28].

It is well known that CeO_2 has redox properties, and participates in the reaction mechanism providing lattice oxygen, which is replaced by oxygen from the gas phase. For this mechanism to occur it is necessary the oxygen in the gas phase, otherwise only a very small amount of soot is gasified. During the reaction runaway, the oxygen concentration in the gas phase is depleted to low levels, but as long as its concentration is not zero, the redox mechanism can occur. Otherwise, if the oxygen concentration is fully depleted, the reaction will be stopped [32].

4.4. Energy transfer limitations

The heating of the catalytic bed due to the exothermicity of the reaction and because of energy transfer limitations is clearly observed in the experiments carried out measuring the bed temperature, as shown as an example in Fig. 7B. An increase of over

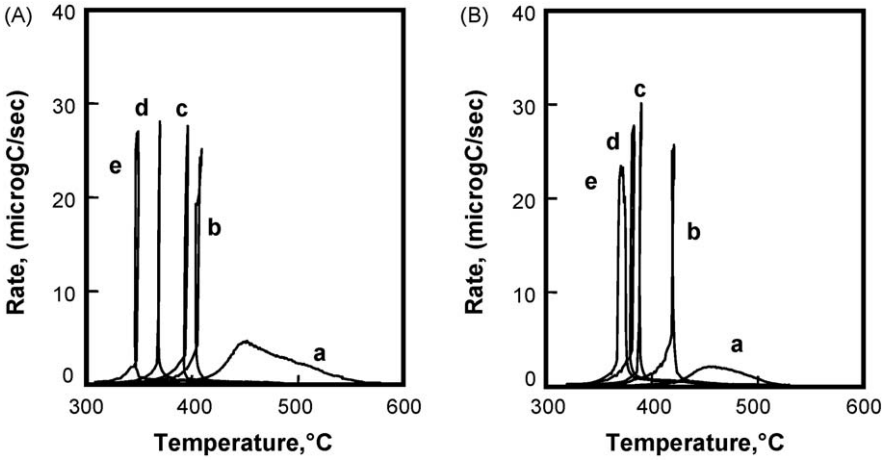

Fig. 11. TPO profiles, (A) KNO_3(4.5)/CeO_2 and (B) KNO_3(4.5)/La_2O_3—(a) carrier 5% O_2/N_2 loose contact. Other curves, carrier 1000 ppm NO in air: (b) loose contact; (c) mixed in a mortar 20 s; (d) mixed in a mortar 60 s, (e) tight contact.

30 °C took place in a very small bed of 10 mg, and moreover, with a thermocouple inside the bed, which leads to a dampening effect of the reaction runaway due to the heat absorption by this temperature sensor.

The apparent shift towards lower temperatures as the catalyst:soot ratio decreases, observed in the experiments carried out with the U-shape reactor (Fig. 3A) is due to the local sample overheating compared to the gas phase. Under this condition, the real sample temperature is higher than that registered by the thermocouple, which is located in a symmetrical arm of the analysis cell, and therefore measuring the gas phase temperature.

It is also interesting to compare the displacements of the DSC and TPO profiles (Figs. 1 and 3, respectively) for the different catalyst–soot ratios. When increasing the catalyst–soot ratio, the DSC profile displaces to lower temperatures, in contrast with what was observed with the TPO experiments. This apparent difference is due only to the temperature sensor position in each case, and is also a clear indication of the phenomena under analysis. In one case (TPO) the local heating of the catalytic bed is not detected by the temperature sensor in the U-shape reactor, while in the other (DSC) the bed temperature is controlled by the power supply during the analysis.

4.5. Surface composition of La_2O_3 supported catalysts and runaway dampening

The effect that the state of the hydroxylated catalytic surface has to avoid the reaction runaway is further supported by the data shown in Figs. 5 and 6. In the former, a runaway can be observed in an incipient way on a freshly calcined lanthanum supported catalyst, while it is not observed after the catalyst was exposed to the environment. In a similar way, Fig. 6 shows additional evidence. The catalyst:soot mixture displays the temperature runaway phenomena in an incipient way when performing the experiment with the dry carrier. Note that the peak displays a spike at the maximum (curve a). The formation of $La(OH)_3$ under the wet carrier contributes even more to the runaway dampening (curve b). Finally, the TPO profile corresponding to the oldest mixture (curve c) is similar to the profile obtained when using the wet carrier (curve b). It has to be recalled that, the older the catalyst, the higher $La(OH)_3$ quantity in the catalyst, as shown by FTIR (Fig. 9) and XRD (Fig. 8). Again, this confirms the $La(OH)_3$ dampening action to avoid the runaway effect. It also confirms that the higher the $La(OH)_3$ amount, the higher the heat absorption due to dehydroxylation and, therefore, the higher the dampening effect.

Depending upon the temperature and the gas phase composition (H_2O, CO_2, NO_x, etc.) the lanthanum surface is partially covered to different extents with CO_2 and adsorbed NO_x (nitrates). As above discussed, CO_2 interacts with lanthanum mainly at high temperatures, such as above 350 °C. However, carbonates decompose between 460 and 550 °C approximately, with a well-defined endothermic peak [12]. If the surface is partially covered with carbonates as expected during a real operation and a runaway takes place, when the catalyst temperature increases above 460 °C, the endothermic decomposition of these compounds will also act dampening the runaway. Nevertheless, data shown in Table 1 indicate that the heat consumed by dehydroxylation while heating the sample in a carrier containing 10% CO_2 is almost the same as when using O_2/N_2 carrier gas, being 128 and 145 J/g, respectively. Similar behavior was observed when burning the soot using the carrier gas with CO_2, being the heat evolved in this case 714 J/g, while it is 702 J/g when using O_2/N_2 carrier gas.

4.6. Effect of contact type and NO in the gas phase

Fig. 11 shows experiments carried out with catalyst:soot mixtures under a loose contact type, both with and without NO in the gas phase. It is interesting to observe, that with 5:1 catalyst:soot mass ratio the system does not display reaction runaway, neither with CeO_2 nor with La_2O_3 supported catalysts using 5% O_2/N_2 carrier gas (curves a in Fig. 11A and B). This occurs because the reaction rate does not reach a threshold value in order to go into a runaway at this catalyst:soot mass ratio. However, when NO is present, the reaction rate increases and the system displays the typical shape of a runaway phenomenon. This occurs both in CeO_2 and La_2O_3 supported catalyst. Nevertheless, a very important difference between both catalysts can be observed. Fig. 11A and B shows experiments carried out with catalyst:soot mixtures with different levels of contact. On one hand, the loose contact obtained just by shaking the soot and the catalysts in a vial, are displayed (curves b). It can be seen that the system displays the runaway. The reaction is taking place outside the temperature range in which the endothermic process takes place in the case of the lanthanum supported catalyst, and therefore the runaway is observed. Experiments were carried out using mixtures of soot and catalyst with increasing contact level. To achieve this, mixtures were prepared as in the tight contact mode, but using very short mixing times. A distinctive feature can be observed in these series of experiments comparing lanthanum and ceria supported catalysts. As the TPO profiles shifts to lower temperatures, and

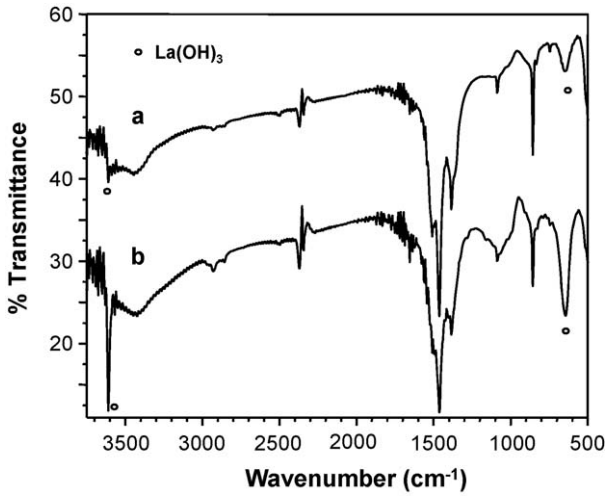

Fig. 12. FTIR spectra of KNO_3/La_2O_3 calcined at 400 °C, (a) fresh; (b) treated with 1000 ppm NO + 10% water, balance air, at 320 °C, during 1 h.

falls into the temperature range in which the endothermic dehydroxylation occurs, different behavior is found. As the soot oxidation shifts to lower temperatures due to a better contact between the solid phases, the lanthanum supported catalyst displays a TPO profile with a decreasing maximum rate and consequently burning the soot in a wider temperature range. On the other hand, the ceria supported catalyst displays a TPO profile that shifts to lower temperatures, but does not become lower in intensity or wider as in the case of lanthanum. This is another very important result, and proves that lanthanum is able to dampen the reaction runaway, decreasing the maximum reaction rate and consequently the maximum temperature reached in the system, also in the presence of NO in the gas phase and a loose contact type.

Fig. 12 shows the FTIR spectra of the fresh K/La_2O_3 catalyst and after being treated with 1000 ppm NO and 10% water at 320 °C. It can be clearly seen that there are hydroxyl groups left on the surface after this treatment, and consequently the endothermic process also occurs when the catalyst is exposed to NO.

4.7. Reaction runaway analysis and the experimental set-up

At this point it is interesting to compare the different experimental set-ups in order to assure that the runaway dampening by lanthanum hydroxides are really taking place. On one hand, DSC and TPO clearly show the fast increase in reaction rate at high soot loading, which is not compatible with a system controlled by a kinetic regime. This is observed with both techniques, even though there are small differences in the experimental conditions, such as the heating rate (10 °C/min for DSC and 12 °C/min for TPO), and carrier composition and flow rate. The reason of this is that the uncontrolled reaction occurs at a given temperature and soot loading, being irrelevant the ramp rate used to reach that stage, or the gas flow rate, as long as the oxygen concentration is enough to burn the soot. On the other hand, we had verified by different TPO configurations, that the bed temperature increases significantly above the gas phase when the reaction accelerates leading to the fast increase in the soot burning rate. Finally, since for this analysis a very fast analytical response is needed and therefore a specific configuration for the total amount of $CO + CO_2$ determination was used, which is the methanation of these compounds. This technique makes it possible to have a continuous and high sensitivity signal, without missing the spikes generated in many cases in the TPO profiles during the runaway, as shown in Section 3.

5. Conclusions

Different techniques and experimental set-ups have been used in this work to demonstrate that a runaway phenomena takes place during soot combustion on ceria supported catalysts at high soot:catalyst mass ratio, while it is not observed under the same conditions on lanthanum supported catalysts. DSC experiments, and the combination of TPO analyses with direct measurement of the catalytic bed temperature, or with measurement of the gas phase temperature, were carried out to obtain information regarding the behavior of these systems.

In summary, the following are the main experimental evidences regarding the runaway dampening capacity of lanthanum supported catalysts:

- XRD and FTIR shows the presence of $La(OH)_3$ in the catalysts that do not display the runaway.
- DSC clearly shows that $La(OH)_3$ decomposes in the same temperature range as the soot is burnt, and this decomposition is endothermic.
- Lanthanum supported catalysts that do not have $La(OH)_3$ (such as when using catalyst recently calcined) have runaway.
- Dehydroxylated catalyst mixed with soot liberates similar amount of heat as ceria supported catalyst.
- There are differences in the extent of the runaway if wet or dry air is used.
- The heat evolved when burning soot with lanthanum supported catalyst is lower than in the case of ceria supported catalysts.
- When using loose contact mixtures, and the soot oxidation occurs out of the temperature range for dehydroxylation on lanthanum, the runaway takes place.

Taking into account the experiments carried out with both catalysts, it can be observed that there is a general tendency of the runaway to occur at high soot loadings in the presence of K/CeO_2 and not in the presence of K/La_2O_3. Even though both catalysts have similar intrinsic activities (at temperatures near those at which the reaction runaway occurs), the coexistence of exothermic and endothermic processes is decisive as far as the runaway is concerned. As the combustion in the presence of K/La_2O_3 proceeds, the $La(OH)_3$ decomposition (with a maximum at 380 °C) also takes place. This endothermic evolution consumes part of the heat released during soot combustion. Even when the heat consumed for the $La(OH)_3$ decomposition is smaller than the heat released during soot combustion, it is enough to damp the reaction runaway. This property is very important under conditions in which eventually, a large quantity of soot could be accumulated on the catalytic filter producing the reaction runaway. In such a situation, the filter with the K/CeO_2 catalyst could fail, while the filter with the K/La_2O_3 catalyst could damp the combustion reaction runaway, thus avoiding the filter failure and increasing its lifetime. An important experimental observation is that the dehydroxylation also occurs in the presence of water in the gas phase, this being a key issue regarding the catalyst behavior exposed to real exhaust gases.

Another important observation is that the precursor used during the catalyst preparation and the pretreatment has an influence in order to avoid the reaction runaway, since both of them modify the relative heat generation–consumption processes, and the temperature at which each process takes place.

This idea can be applied for catalyst design with an improved stability due to a self-protection against reaction runaway, by choosing supports for the active phase that display endothermic phase transitions in the same temperature range as the soot combustion.

Acknowledgments

The authors wish to acknowledge the financial support received from UNL and ANPCyT. Thanks are given to Elsa Grimaldi for the edition of the English manuscript, and to Ana Belén Patiño for her technical assistance.

References

[1] Y. Watabe, K. Irako, T. Miyajima, T. Yoshimoto, Y. Murakami, S. A. E. Spec. Publ., S. A. E. 830082 (1983) 45.
[2] M.A. Peralta, V.G. Milt, L.M. Cornaglia, C.A. Querini, J. Catal. 242 (2006) 118.
[3] Z. Zhang, Z. Mou, P. Yu, Y. Zhang, X. Ni, Catal. Commun. 8 (2007) 1621.
[4] R. Jiménez, X. García, C. Cellier, P. Ruiz, A.L. Gordon, Appl. Catal. A: Gen. 314 (2006) 81.
[5] P.A.J. Neeft, M. Makkee, J.A. Moulijn, J. Chem. Eng. 64 (1996) 295.
[6] Z. Zhao, A. Obuchi, J. Oi-Uchisawa, A. Ogata, S. Kushiyama, Chem. Lett. 4 (1998) 367.
[7] E. Aneggi, C. de Leitenburg, G. Dolcetti, A. Trovarelli, Catal. Today 136 (2008) 3.
[8] Minnesota Mining and Manufacturing Company. Patent 5656048 (1997).
[9] Haldor Topsoe A/S. Patent 5884474 (1999).
[10] Fleetguard, Inc. Patent 7377101 (2008).
[11] Peugeot Citroen Automobiles SA. Patent 7225611 (2007).
[12] V.G. Milt, C.A. Querini, E.E. Miró, Thermochim. Acta 404 (2003) 177.
[13] C.A. Querini, M.A. Ulla, F. Requejo, J. Soria, U.A. Sedrán, E.E. Miró, Appl. Catal. B: Environ. 15 (1998) 5.
[14] J.P.A. Neeft, O.P. Van Pruissen, M. Makkee, J.A. Moulijn, St. Surf. Sc. Catal. 96 (1995) 549.
[15] B.A.A.L. van Setten, J.M. Schouten, M. Makkee, J.A. Moulijn, Appl. Catal. B 28 (2000) 253.
[16] S.C. Fung, C.A. Querini, J. Catal. 138 (1992) 240.
[17] C.A. Querini, S.C. Fung, Appl. Catal. A: Gen. 117 (1994) 53.
[18] P. Ciambelli, P. Corbo, M. Gambino, V. Palma, S. Vaccaro, Catal. Today 27 (1996) 99.
[19] J.P.A. Neeft, T.X. Nijhuis, E. Smakman, M. Makkee, J.A. Moulijn, Fuel 76 (1997) 1129.
[20] C. Li, T.C. Brown, Carbon 39 (2001) 725.
[21] F. Larachi, K. Belkacemi, S. Hamoudi, A. Sayari, Catal. Today 64 (2001) 163.
[22] D. Fino, P. Fino, G. Saracco, V. Specchia, Appl. Catal. B: Environ. 43 (2003) 243.
[23] G.A. Stratakis, A.M. Stamatelos, Combust. Flame 132 (2003) 157.
[24] A. Yezerets, N.W. Currier, D.H. Kim, H.A. Eadler, W.S. Epling, C.H.F. Peden, Appl. Catal. B: Environ. 61 (2005) 120.
[25] M.N. Bokova, C. Decarne, E. Abi-Aad, A.N. Ptykhin, V.V. Lunin, A. Aboukäis, Thermochim. Acta 428 (2005) 165.
[26] T.J. Keskitalo, K.J.T. Lipiäinen, A.O.I. Krause, Chem. Eng. J. 120 (2006) 63.
[27] P. Darcy, P. Da Costa, H. Mellottée, J.M. Trichard, G. Djéga-Mariadassou, Catal. Today 119 (2007) 252.
[28] M.A. Peralta, M.S. Gross, B. Sanchez, C.A. Querini, Chem. Eng. J. 152 (1) (2009) 234–241.
[29] V.G. Milt, M.L. Pisarello, C.A. Querini, E.E. Miró, Appl. Catal. B: Environ. 41 (2003) 397.
[30] M.A. Peralta, Doctoral Thesis: Diesel Exhausts Gases Pollutants Abatment: Catalysts Stability, Universidad Nacional del Litoral, Argentina, 2007.
[31] R.P. Taylor, G.L. Schrader, Ind. Eng. Chem. Res. 30 (5) (1991) 1016.
[32] G. Mul, F. Kapteijn, C. Doornkamp, J.A. Moulijn, J. Catal. 179 (1998) 258.